Metabolism and DNA repair Shape a Specific Modification Pattern in Mitochondrial DNA

[1]Tina Pawar, [2,3]Magnar Bjørås, [2]Arne Klungland and [1]Lars Eide*

[1]Department of Medical Biochemistry, [2]Department of Microbiology, University of Oslo and Oslo University Hospital, Rikshospitalet, 0372 Oslo, Norway

[3]Department of clinical and Molecular Medicine, Norwegian University of Science and Technology, Trondheim, Norway

*To whom correspondence should be addressed:

Lars Eide, Dept. Medical Biochemistry, B1.3054, Rikshospitalet, Sognsvannsveien 20, 0372 Oslo, Norway. Email: lars.eide@medisin.uio.no

Phone: +47 23071062

FIGURE 1

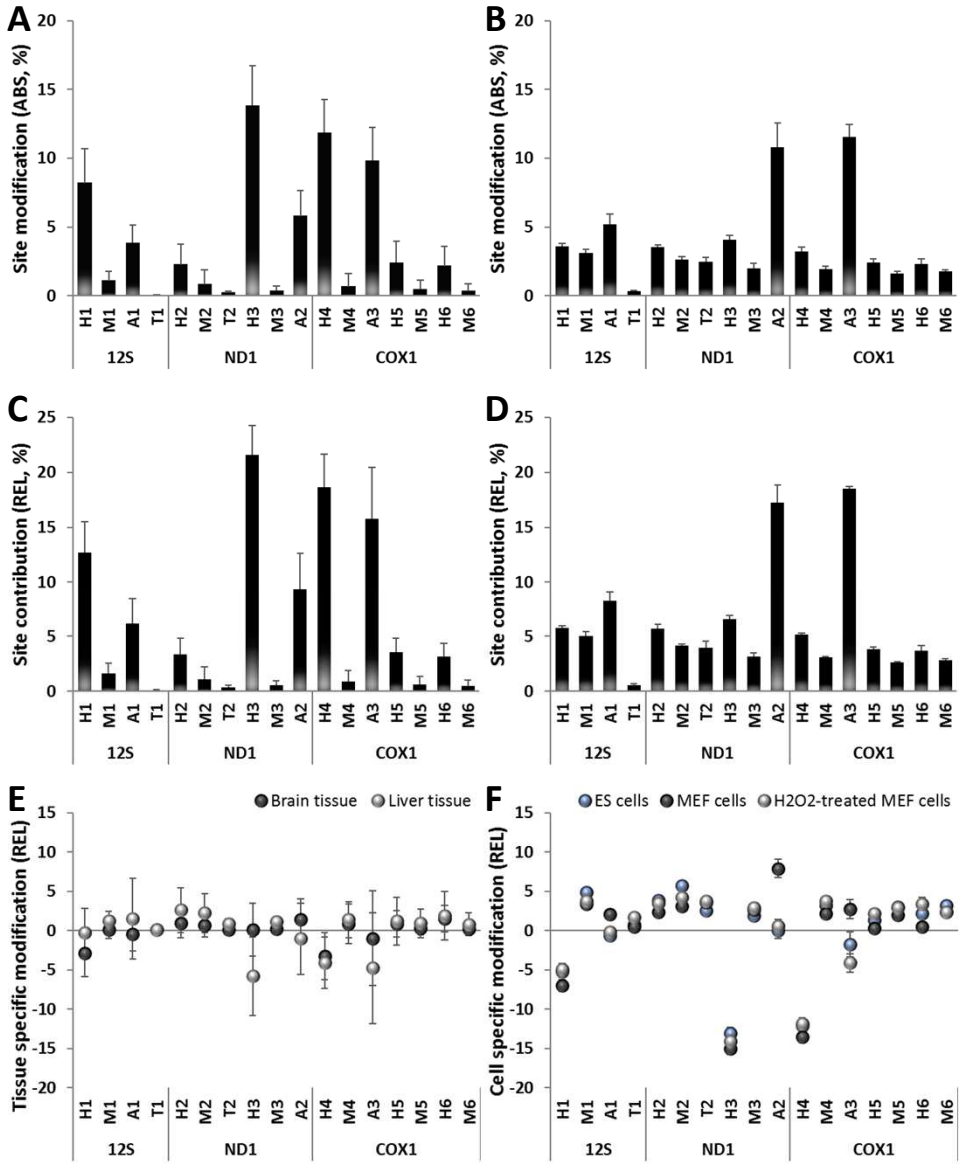
A
Site modification (ABS, %)
B
Site modification (ABS, %)
C
Site contribution (REL, %)
D
Site contribution (REL, %)
E
Brain tissue
Liver tissue
Tissue specific modification (REL)
F
ES cells
MEF cells
H2O2-treated MEF cells
Cell specific modification (REL)
H1 M1 A1 T1 H2 M2 T2 H3 M3 A2 H4 M4 A3 H5 M5 H6 M6
12S
ND1
COX1

FIGURE 2

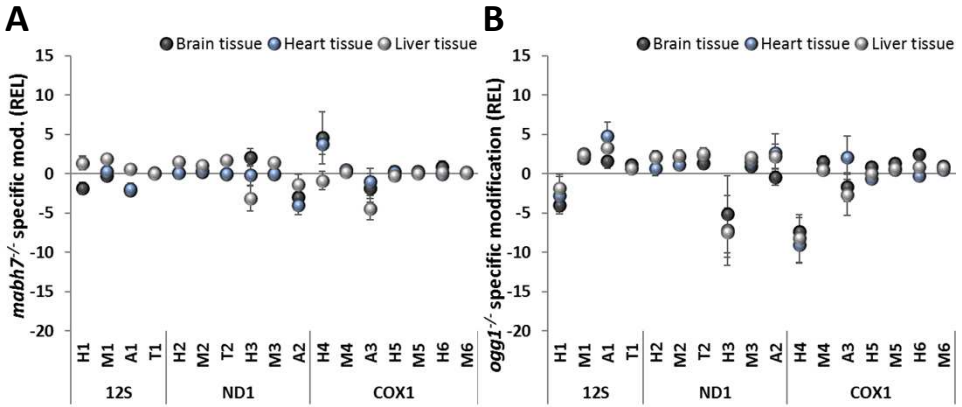
A
B
Brain tissue
Heart tissue
Liver tissue
mabh7-/- specific mod. (REL)
ogg1-/- specific modification (REL)
15
10
5
0
-5
-10
-15
-20
H1
M1
A1
T1
H2
M2
T2
H3
M3
A2
H4
M4
A3
H5
M5
H6
M6
12S
ND1
COX1

FIGURE 3

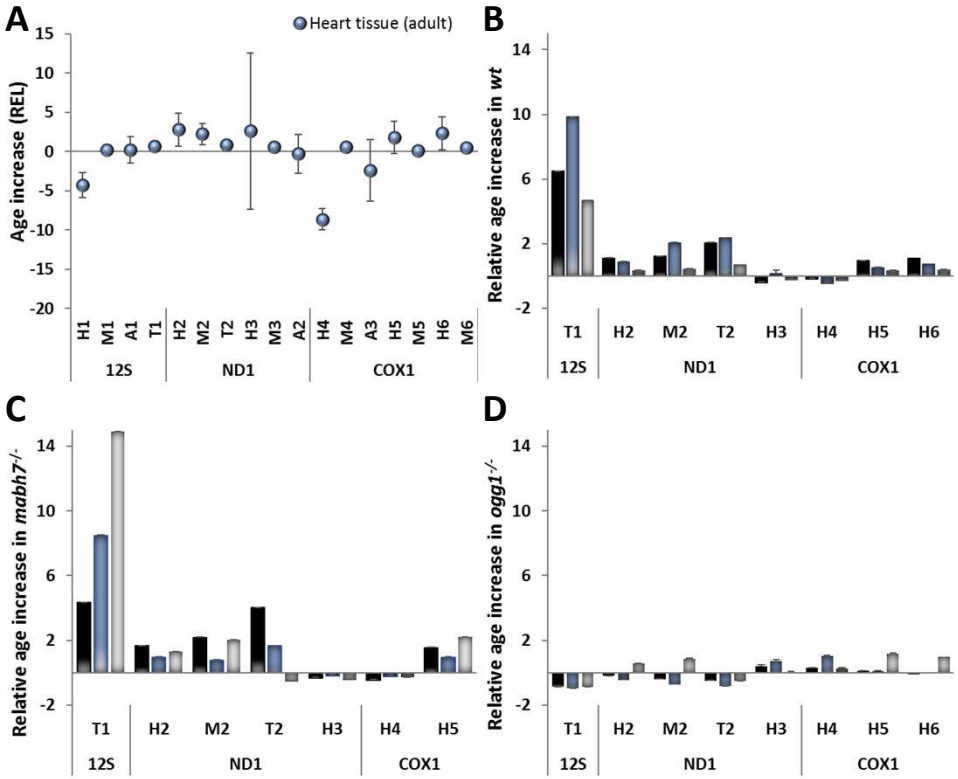
A
Heart tissue (adult)
Age increase (REL)
15
10
5
0
-5
-10
-15
-20
H1 M1 A1 T1 H2 M2 T2 H3 M3 A2 H4 M4 A3 H5 M5 H6 M6
12S
ND1
COX1
B
Relative age increase in wt
14
10
6
2
-2
T1 H2 M2 T2 H3 H4 H5 H6
12S
ND1
COX1
C
Relative age increase in mdbh7-/-
14
10
6
2
-2
T1 H2 M2 T2 H3 H4 H5
12S
ND1
COX1
D
Relative age increase in ogg1-/-
14
10
6
2
-2
T1 H2 M2 T2 H3 H4 H5 H6
12S
ND1
COX1

FIGURE 4

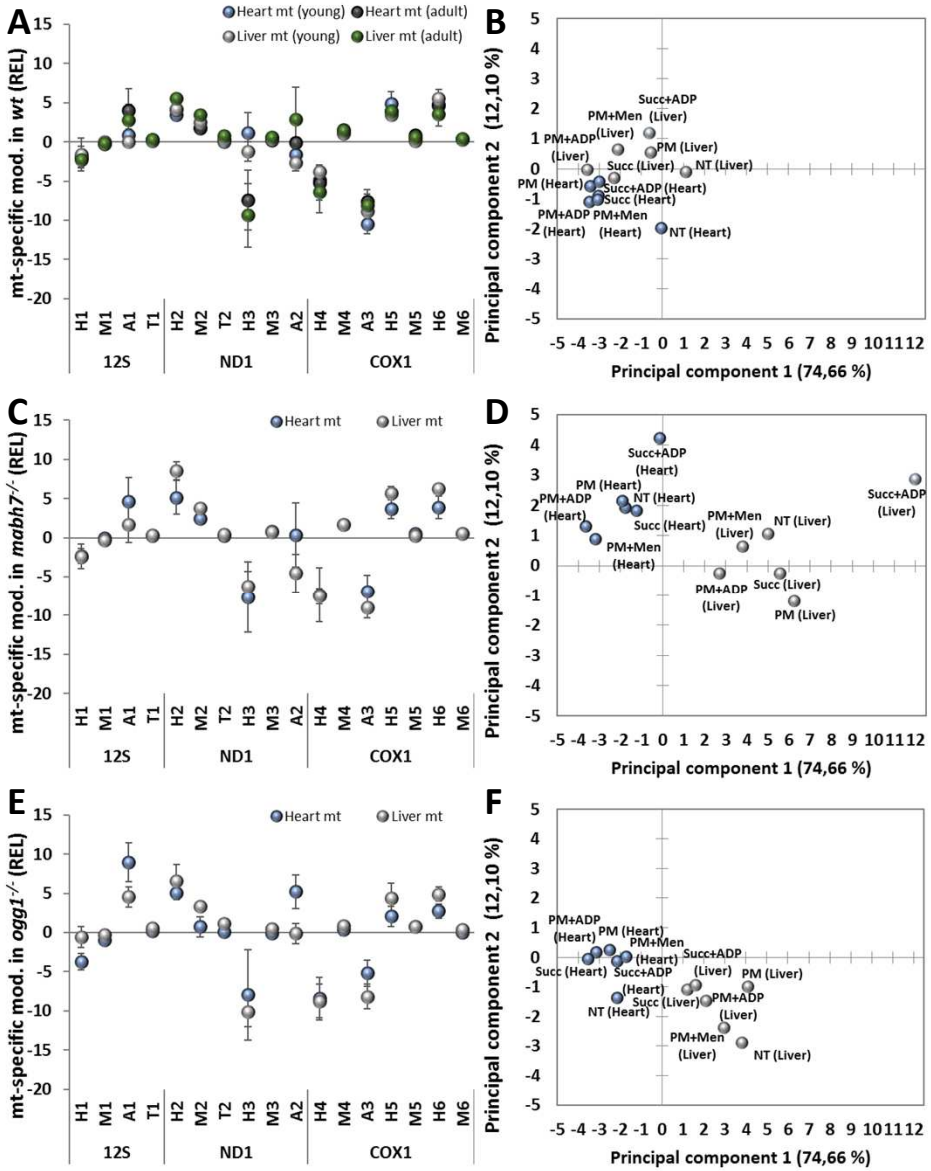
A
Heart mt (young)
Heart mt (adult)
Liver mt (young)
Liver mt (adult)
mt-specific mod. in wt (REL)
H1 M1 A1 T1 H2 M2 T2 H3 M3 A2 H4 M4 A3 H5 M5 H6 M6
12S
ND1
COX1
B
Principal component 2 (12,10 %)
Principal component 1 (74,66 %)
Succ+ADP (Liver)
PM+Men (Liver)
PM+ADP (Liver)
PM (Liver)
Succ (Liver)
NT (Liver)
PM (Heart)
Succ+ADP (Heart)
Succ (Heart)
PM+ADP (Heart)
PM+Men (Heart)
NT (Heart)
C
Heart mt
Liver mt
mt-specific mod. in mabh7-/- (REL)
D
Succ+ADP (Heart)
PM (Heart)
PM+ADP (Heart)
NT (Heart)
Succ (Heart)
PM+Men (Heart)
Succ+ADP (Liver)
PM+Men (Liver)
NT (Liver)
PM+ADP (Liver)
Succ (Liver)
PM (Liver)
E
Heart mt
Liver mt
mt-specific mod. in ogg1-/- (REL)
F
PM+ADP (Heart)
PM (Heart)
PM+Men (Heart)
Succ (Heart)
Succ+ADP (Heart)
Succ+ADP (Liver)
PM (Liver)
Succ (Liver)
PM+ADP (Liver)
NT (Heart)
PM+Men (Liver)
NT (Liver)

FIGURE 5

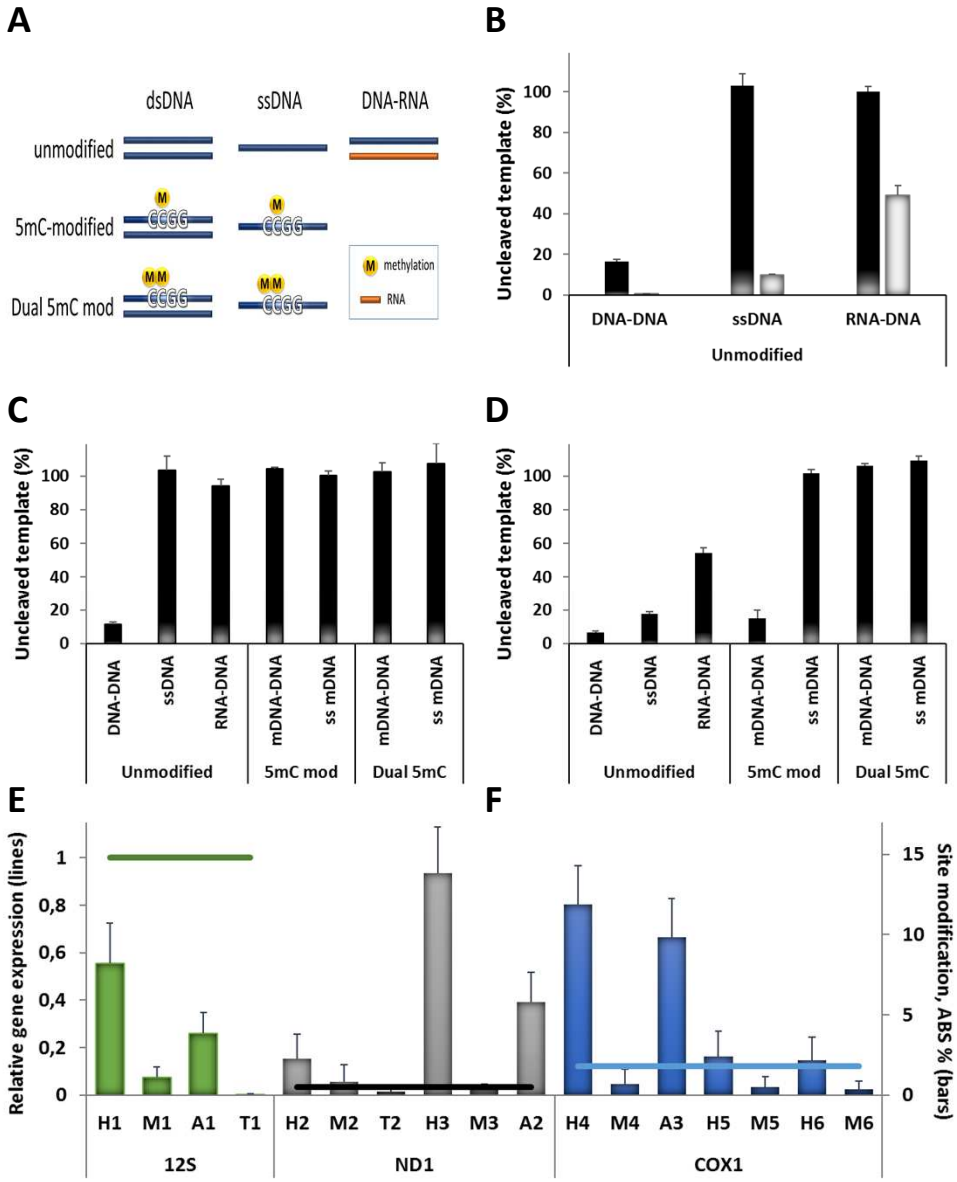
A
dsDNA
ssDNA
DNA-RNA
unmodified
5mC-modified
Dual 5mC mod
CCGG
methylation
RNA
B
Uncleaved template (%)
DNA-DNA
ssDNA
RNA-DNA
Unmodified
C
Uncleaved template (%)
DNA-DNA
ssDNA
RNA-DNA
mDNA-DNA
ss mDNA
mDNA-DNA
ss mDNA
Unmodified
5mC mod
Dual 5mC
D
Uncleaved template (%)
DNA-DNA
ssDNA
RNA-DNA
mDNA-DNA
ss mDNA
mDNA-DNA
ss mDNA
Unmodified
5mC mod
Dual 5mC
E
F
Relative gene expression (lines)
Site modification, ABS % (bars)
H1 M1 A1 T1 H2 M2 T2 H3 M3 A2 H4 M4 A3 H5 M5 H6 M6
12S
ND1
COX1

FIGURE 6

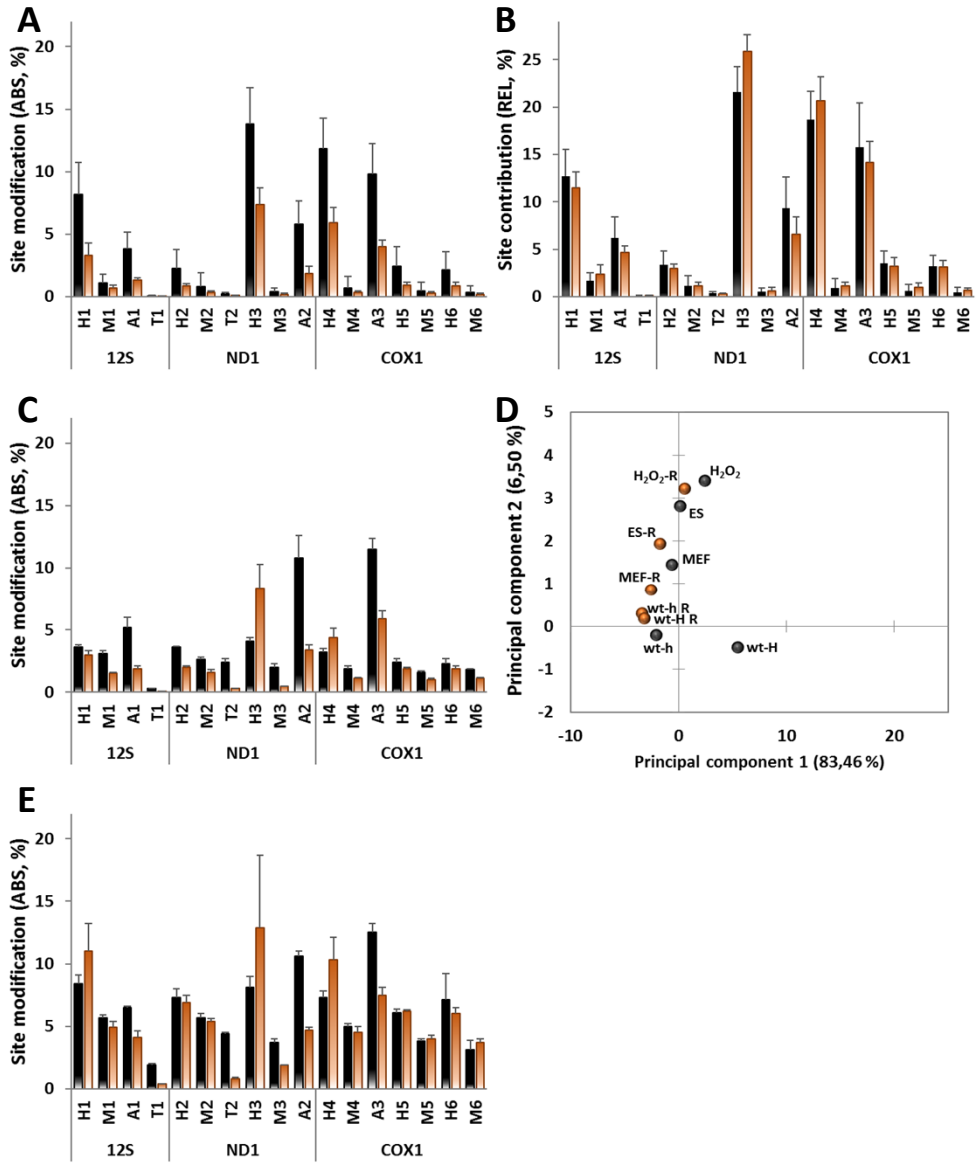
A
Site modification (ABS, %)
0
5
10
15
20
H1 M1 A1 T1 H2 M2 T2 H3 M3 A2 H4 M4 A3 H5 M5 H6 M6
12S
ND1
COX1
B
Site contribution (REL, %)
0
5
10
15
20
25
H1 M1 A1 T1 H2 M2 T2 H3 M3 A2 H4 M4 A3 H5 M5 H6 M6
12S
ND1
COX1
C
Site modification (ABS, %)
0
5
10
15
20
H1 M1 A1 T1 H2 M2 T2 H3 M3 A2 H4 M4 A3 H5 M5 H6 M6
12S
ND1
COX1
D
Principal component 2 (6,50 %)
5
4
3
2
1
0
-1
-2
-10
0
10
20
Principal component 1 (83,46 %)
H2O2-R
H2O2
ES
ES-R
MEF
MEF-R
wt-h R
wt-H R
wt-h
wt-H
E
Site modification (ABS, %)
0
5
10
15
20
H1 M1 A1 T1 H2 M2 T2 H3 M3 A2 H4 M4 A3 H5 M5 H6 M6
12S
ND1
COX1

FIGURE 7

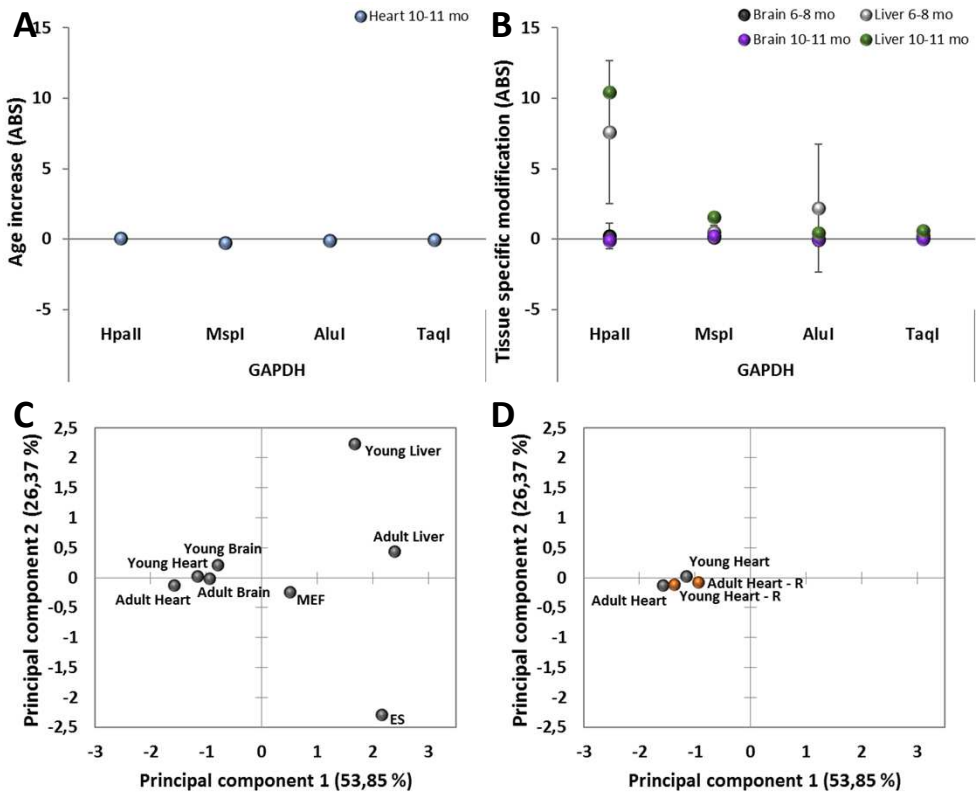
A
Heart 10-11 mo
Age increase (ABS)
15
10
5
0
-5
HpaII
MspI
AluI
TaqI
GAPDH
B
Brain 6-8 mo
Liver 6-8 mo
Brain 10-11 mo
Liver 10-11 mo
Tissue specific modification (ABS)
15
10
5
0
-5
HpaII
MspI
AluI
TaqI
GAPDH
C
Principal component 2 (26,37 %)
2,5
2
1,5
1
0,5
0
-0,5
-1
-1,5
-2
-2,5
Young Liver
Adult Liver
Young Brain
Young Heart
Adult Heart
Adult Brain
MEF
ES
-3
-2
-1
0
1
2
3
Principal component 1 (53,85 %)
D
Principal component 2 (26,37 %)
2,5
2
1,5
1
0,5
0
-0,5
-1
-1,5
-2
-2,5
Young Heart
Adult Heart - R
Adult Heart
Young Heart - R
-3
-2
-1
0
1
2
3
Principal component 1 (53,85 %)

FIGURE 8

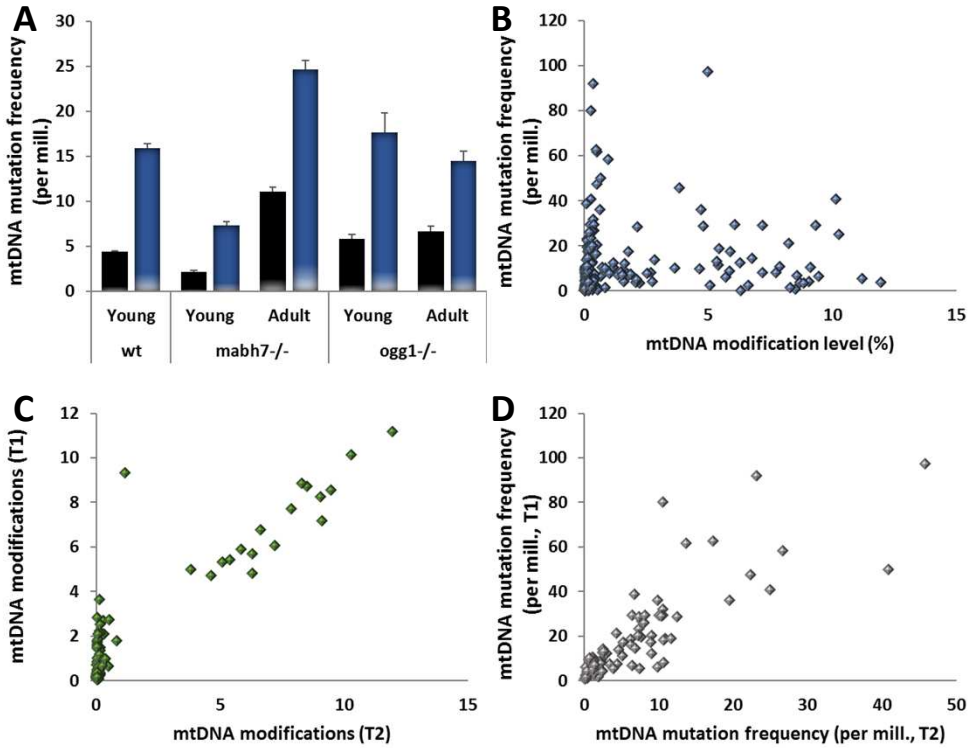
A
mtDNA mutation frecuency (per mill.)
30
25
20
15
10
5
0
Young
Young
Adult
Young
Adult
wt
mabh7-/-
ogg1-/-
B
mtDNA mutation frequency (per mill.)
120
100
80
60
40
20
0
0
5
10
15
mtDNA modification level (%)
C
mtDNA modifications (T1)
12
10
8
6
4
2
0
0
5
10
15
mtDNA modifications (T2)
D
mtDNA mutation frequency (per mill., T1)
120
100
80
60
40
20
0
0
10
20
30
40
50
mtDNA mutation frequency (per mill., T2)

Table 1 - Sample groups used in the study

Total DNA analysis							
Genotype	**Age, months**	**Tissue**			**No. of males**	**No of females**	**Total**
		Brain	**Heart**	**Liver**			
wildtype	6-8	x	x	x	6	9	15
	10-11	x	x	x	3	3	6
alkbh7$^{-/-}$	6	x	x	x	4	0	4
	11	x	x	x	3	5	8
ogg1$^{-/-}$	6-8	x	x	x	3	0	3
	10	x	x	x	0	3	3
In vitro mitochondrial respiration							
Genotype	**Age, months**	**Tissue**			**No. of males**	**No of females**	**Total**
		Brain	**Heart**	**Liver**			
wildtype	6		x	x	3	0	3
	12		x	x	1	2	3
alkbh7$^{-/-}$	11		x	x	1	0	1
	12		x	x	2	0	2
ogg1$^{-/-}$	6		x	x	3	0	3

Table 2 - Primers used in the study

Name	5'-3' sequence	Sense or antisense	mtDNA Binding site	Used for site
12S.1 for	aggtttggtcctggccttat	sense	72	H1, M1, A1
12S.1 rev	gtggctaggcaaggtgtctt	antisense	221	H1, M1, A1
12S.2 for	actcaaaggacttggcggta	sense	582	T1
12S.2 rev	agcccatttcttcccatttc	antisense	788	T1
ND1.1 for	cacttattacaacccaagaacaca	sense	3241	H2, M2
ND1.1 rev	gcgtattctacgttaaaccctga	antisense	3397	H2, M2
ND1.2 for	ttcgacctgacagaaggagaa	sense	3342	H3, M3, A2
ND1.2 rev	gatgctcggatccataggaa	antisense	3577	H3, M3, A2
ND1.3 for	ttacttctgccagcctgacc	sense	3270	T2
ND1.3 rev	gctataaagaataacgcgaatgg	antisense	3427	T2
COX1.1 for	agaagcaggagcaggaacag	sense	5681	H4, M4, A3
COX1.1 rev	gttatggctgggggtttcat	antisense	5857	H4, M4, A3
COX1.2 for	tttgggcacccagaagttta	sense	6039	H5, M5
COX1.2 rev	tgaatatgtggtgggctcat	antisense	6207	H5, M5
COX1.3 for	tgagcccaccacatattcac	sense	6189	H6, M6
COX1.3 rev	ccggttagaccaccaactgt	antisense	6391	H6, M6

Table 3 - Synthetic oligonucleotides used in the study

Name	5'-3' sequence	Modification	Used for
DNA oligo1a	gaggtttggtcctggccttatagctccggtcgaaagaca ccttgcctagccacg	None	ssDNA, dsDNA and RNA-DNA enzyme activity testing
DNA oligo1b	cgtggctaggcaaggtgtctttcgaccggagctataagg ccaggaccaaacctc	None	Complementary strand to oligo1a
RNA oligo	cguggcuaggcaaggugucuuucgaccggagcuau aaggccaggaccaaaccuc	None	Complementary strand to oligo1a
DNA oligo2a	gaggtaaaattacacatgcaaacctccatagaXXggtg taaaatcccttaaacatttacttaaaatttaaggagaggg	X = 5-Methyl-dC	Hemi-methylated substrate for enzyme activity testing
DNA oligo2b	gaggtaaaattacacatgcaaacctccatagacXggtgt aaaatcccttaaacatttacttaaaatttaaggagaggg	C = 5-Methyl-dC	Hemi-methylated substrate for enzyme activity testing
DNA oligo2c	ccctctccttaaattttaagtaaatgtttaagggattttacac cggtctatggaggtttgcatgtgtaattttacctc	None	Complementary strand to oligo2a and 2b

Table 4 - Site-specific changes in modification (p<0.003)

Heart wildtype vs.		**H1**	**M1**	**A1**	**T1**	**H2**	**M2**	**T2**	**H3**	**M3**	**A2**	**H4**	**M4**	**A3**	**H5**	**M5**	**H6**	**M6**
Wildtype	Brain	÷										÷					+	
	Liver		+			+	+	+	÷	+		÷						
	MEF cells	÷	+		+		+	+	÷	+	+	÷	+			+		+
	H_2O_2- MEF		+		+	+	+	+	÷	+		÷	+			+	+	+
	ES cells	÷	+		+	+	+	+	÷	+		÷	+			+	+	+
Wildtype vs.		**H1**	**M1**	**A1**	**T1**	**H2**	**M2**	**T2**	**H3**	**M3**	**A2**	**H4**	**M4**	**A3**	**H5**	**M5**	**H6**	**M6**
Alkbh7(-/-)	Brain											+						
	Heart																	
	Liver																	
Ogg1(-/-)	Brain				+													
	Heart		+	+	+			+		+		÷						
	Liver							+										
Age effect		**H1**	**M1**	**A1**	**T1**	**H2**	**M2**	**T2**	**H3**	**M3**	**A2**	**H4**	**M4**	**A3**	**H5**	**M5**	**H6**	**M6**
Wildtype	Brain				+	+	+	+	+						+		+	
	Heart				+			+				+						
	Liver																	
Alkbh7(-/-)	Brain					+						+			+		+	
	Heart	+	+															
	Liver	+	+		+	+	+	+	+		+	+	+	+	+		+	+
Ogg1(-/-)	Brain																	
	Heart																	
	Liver																	

Abstract

The mitochondrial DNA (mtDNA) resides in the vicinity of energy-rich reactions. Thus, chemical modifications of mtDNA might mirror mitochondrial processes and could serve as biomarkers of metabolic processes in the mitochondria. This hypothesis was tested by assessing modifications at 17 different sites in the mtDNA as a function of cell type, oxidative stress and mitochondrial activity. Two mouse mutants with a metabolic phenotype were compared to wild-type (WT) mice: the *ogg1*$^{-/-}$ mouse that lacks the 8-oxoguanine DNA glycosylase (OGG1), and the *alkbh7*$^{-/-}$ mouse missing the ALKBH7 protein that has been implicated in fatty acid oxidation. It was found that cell type, oxidative stress and mitochondrial complex activity shaped distinct modification patterns in mtDNA, and that OGG1 and ALKBH7 independently modulated these modification patterns. The modifications included ribonucleotides, which also accumulated in mtDNA with age. Interestingly, this age-dependent accumulation most likely involves DNA repair, as mtDNA from *ogg1*$^{-/-}$ mice did not accumulate modifications with age. On the other hand, *alkbh7*$^{-/-}$ mtDNA accumulated more modifications with age than WT mtDNA. Our results show that mtDNA is dynamically modified with metabolic activity and imply a novel synergy between metabolism and mtDNA repair proteins.

Keywords: mtDNA, OGG1, ALKBH7, DNA modification, metabolism

1. Introduction

The mtDNA is a circular, multicopy genome of 16.6 kb in mammals and resides in the same organelle that hosts high energy-converting redox reactions in the cell. Reactive metabolites have sufficient energy to modify mtDNA. Previous studies have consistently reported more oxidized base lesions in mtDNA than in nuclear DNA, supporting the assumption that lesions accumulate preferentially in mtDNA [1, 2]. Additionally, genotoxins exposed to cells predominantly target mtDNA as compared to nuclear DNA and indicate that the mtDNA itself is more prone to modifications from environmental stimuli [3]. The increased sensitivity of mtDNA to oxidation has been explained by the absence of histone-dependent organization of DNA in the mitochondria. However, mtDNA forms assemblies with proteins and cardiolipin in chromatin-like structures known as nucleoids [4]. Proteomic analyses with isolated mtDNA-bound fractions from various sources have identified metabolic enzymes, electron transport chain components, transcription factors, replication factors and heat shock/chaperone proteins to this structure [5]. The heterologous arrangement of mtDNA implies that changes on the mtDNA can be sensed by proteins involved in many different metabolic processes- or vice versa that metabolic processes generate modifications in the mtDNA characteristic of the ongoing process.

Emerging results imply that DNA repair has strong implications for metabolism. The OGG1 DNA glycosylase participates in nuclear and mitochondrial base excision repair (BER) and the *ogg1*$^{-/-}$ mouse accumulate mtDNA damage, suffers from hyperglycemia, hyperinsulinemia and diet-induced obesity [6, 7]. Another mitochondrial DNA glycosylase, NEIL1, maintains mtDNA and protects against high fat diet-induced metabolic alteration as well [7]. Other mtDNA repair functions like CSB and Ape1 have been associated with metabolic regulations [8, 9], and together imply that there is a mechanistic link between metabolic activity and (mt)DNA maintenance.

The *E.coli* AlkB protein repairs methylated DNA bases, while the many mammalian homolog's have different roles in regulating methyl modifications. The ALKBH7 protein resides in the mitochondria and is associated with fatty acid oxidation [10]. Although the molecular activity of ALKBH7 is still unknown, the mouse mutant weighs more and develops obesity when fed on high fat diet, reminiscent of *neil1*$^{-/-}$ and *ogg1*$^{-/-}$ mice. It was additionally found that the *alkbh7*$^{-/-}$ mice exhibited a specific carbohydrate-dependent altered respiration capacity [10].

Since mtDNA is vulnerable to damage from neighbouring metabolic processes, we hypothesize that it is modified in a manner that reflects the metabolic activity of the organelle. The assembly of metabolic proteins and mtDNA in the nucleoid might produce a sequence-specific modification of mtDNA. Different tissues have a distinct mitochondrial composition [11], thus we postulated that the mtDNA modifications would be induced in a tissue specific manner as well as correlating with other metabolism-influencing factors like age, oxidative stress and genotype. The *ogg1*$^{-/-}$ and *alkbh7*$^{-/-}$ mutants represent interesting models in this respect.

We previously identified modification frequency in mtDNA [12] at a level that exceeds previous estimates (~$5x10^{-4}$ per nt) of the major lesion 8-oxoguanine [6, 13]. The modifications are detected by the ability to inhibit DNA restriction enzyme digestion. The method has been used to quantify epigenetic marks of DNA, and although mitochondrial epigenetics is still enigmatic [14], the method can be used to characterize DNA integrity in general. The identity of underlying mtDNA modifications can be explored by nucleic acid-modifying enzymes.

Here, we have used a combination of molecular biology methods and statistical analyses to evaluate possible correlation between mitochondrial processes and mtDNA. Our findings unravel new sides of mtDNA and its continuous processes that revitalize the role of mtDNA repair.

2. Materials and methods

2.1. Mice, cell, cultivation

Mouse embryonic fibroblast (MEF) cells were cultured in 95% air and 5% CO2 using high glucose Dulbecco's Modified Eagle Medium (DMEM) with 10 % FBS, 1% Penicillin/Streptomycin and 1% Glutamine. Treatments were carried out at 70-80 % confluence with 50 μM H2O2 for 15 minutes, and the cells were subsequently washed with PBS, trypsinated and pelleted at 2000 rpm.

Embryonic stem (ES) cells were grown in same atmosphere and DMEM (high glucose), 10% knockout serum replacement, 2mM GlutaMaxT, 1% MEM non-essential amino acid solution, 0.5% N2 supplement, 0.1mM β-mercaptoethanol, 1% penicillin/streptomycin, leukemia inhibitoryfactor (LIF: 1000 units/ml) and basal fibroblast growth factor (bFGF: 5ng/ml).

Wild type (WT) mice were c57/Bl/6N. In addition, *alkbh7*$^{-/-}$ and *ogg1*$^{-/-}$ mice were in-house stock. An overview of the material used is given in Table 1. The animal projects in charge of A. Klungland (WT/*alkbh7*$^{-/-}$) and M. Bjørås (WT/*ogg1*$^{-/-}$) were approved by the Norwegian Animal Research Authority and in accordance with the laws and regulations controlling experimental procedures in Norway and the European Union's Directive 86/609/EEC.

2.2. Isolation of mitochondria, mitochondrial activation

Crude heart and liver mitochondria were purified by differential centrifugation, modified from [15]. Fresh tissue was homogenized in 1mL mitochondrial isolation buffer, 1X MSHE buffer (0.21 M mannitol, 0.07 M sucrose, 10 mM Hepes (pH 7.4), 1 mM EDTA, 1 mM EGTA), using a 1mL homogenizer (4 strokes with A pestle (0.1 mm clearance) + 8 strokes with B pestle (0.05 mm clearance) and subsequent purification by differential centrifugation. The mitochondrial pellet was washed twice in 1xMSHE (resuspended in 1 mL and re-pelleted at 10.000 g / 10min).

For mitochondrial activation, the pelleted mitochondria were resuspended in 1X mitochondrial respiration buffer (Mir05 buffer: alexand/gnaiger) 20 mM HEPES, 10 mM KH_2PO_4, 110 mM D-sucrose, 20 mM taurine, 60 mM K-lactobionate, 0.5 mM EGTA, 3 mM $MgCl_2$, 1 g/l fatty acid-free BSA) and incubated for 20 min at 37° with different substrates: complex I substrates: pyruvate (5 mM) + malate (2 mM) with and without ADP (1mM) (PM/PM+ADP); complex II substrates. succinate (10 mM) with and without ADP (1mM) (Succ/Succ+ADP); and electron uncoupler: menadione (0.1mM in the presence of PM). After

completed incubation the mitochondria were pelleted and stored at -80°C prior to DNA isolation.

2.3. Nucleic acid isolation, gene expression analysis

For isolation of total DNA, tissue was collected and stored for 24-48 h in RNAlater® at 4°C before being homogenised and stored at -80°C. Total DNA was isolated using the DNeasy Blood & Tissue Kit (Qiagen, Hilden, Germany) according to the manufacturer's description. DNA isolation from cells and purified mitochondria was performed similarly except that RNAlater was omitted.

2.4. RNA isolation

Total RNA was isolated using RNeasy Mini Kit (Qiagen), according to the manufacturer's description. cDNA was synthesised from isolated total RNA using QuantiTect Reverse Transcription Kit (Qiagen). Gene expression was measured using all the same primer sets as for mtDNA modification analysis.

2.5. mtDNA modification analysis

The qPCR method to characterize mtDNA modifications was established previously [16] and is based on the ability of DNA damage to inhibit Taq$^{\alpha}$I restriction enzymes cleavage. Here, the method is expanded to capture 17 restriction enzyme sites, in three mitochondrial genes. 60 ng of DNA was digested with 10 units of either HpaII, MspI, AluI or Taq$^{\alpha}$I (New England Biolabs) in 1X CutSmart Buffer at 37°C (65°C for Taq$^{\alpha}$I) for 1 hour in a total volume of 20 uL and heat inactivated at 80°C for 30 minutes. Nomenclature and gene position of the the 17 sites: H1 denotes HpaII site no.1, M1 MspI site no1 etch. The sites H1, M1, A1 and T1 resides in the *mt-Rnr1* gene of mtDNA, while H2, M2, T2, H3, M3 and A2 is located in the *mt-Nd1* gene and H4, M4, H5, M5, H6 and M6 harbour in the *mt-Cox1* gene.

For removal of ribonucleotides prior to analyses, DNA was incubated at 37°C for 1 hour with 10 units of either RNase I_f (New England Biolabs) in 1X NEBuffer 3 followed by heat inactivation at 70°C for 30 minutes.

DNA (1.8 ng) was mixed with Power SYBR Green PCR Master Mix (Life Technologies, Carlsbad, CA). Applied Biosystems StepOnePlus™ RealTime PCR System (Applied Biosystems, Waltham, MA) was used for qPCR analysis with the following conditions: Initial denaturation at 95 ºC for 10 minutes followed by 40 cycles of 95 ºC for 15 seconds and 60 ºC for 1 minute.

The absolute modification level was calculated using the following formula: $1/2^{\Delta Ct}$, of which $\Delta Ct = Ct_{\text{treated DNA}} - Ct_{\text{non-treated DNA}}$ (treated = restriction enzyme treatment). The relative modification values were obtained for each site by the following formula: site modification / total sum of modification for all 17 sites. Cumulative values represent the sum of all 17 sites.

2.6. mtDNA mutation analysis

The mtDNA mutation frequency was determined in the T1 and T2 sites, as described previously [17].

2.7. Oligonucleotides

The primers used are supplied in Table 2, and were purchased from Eurofins Genomics.

Modified oligonucleotides (containing modified cytosines or ribonucleotides) were from Eurofins Genomics and are provided in Table 3. Annealing of complementary oligonucleotides was carried out in 1X UltraPure SSC buffer (Thermo Fisher Scientific) in a thermal cycler with the following conditions: 95 ºC for 5 minutes followed by a temperature decrease of 0.1ºC pr. second until 20ºC was reached.

2.8. Statistical analyses

Students T-test was used to check for statistical significance between sample groups using a Bonferroni corrected p-value for multiple testing ($p \leq 0.003$). Correlation analysis was carried out in SPSS using Spearman correlation analysis. Principle component analyses were performed to characterize hierarchal groups. All groups were included in the calculations to provide similar component reference, after where selected groups were presented separately to allow better comparisons. The majority of the variation was found in the first component (>90%).

3. Results

3.1. Cell- and condition- specific mtDNA modification pattern

Mitochondrial DNA modifications were determined by a previously established qPCR-based quantitative assay that senses the ability of DNA modifications to inhibit restriction enzyme cleavage. Four different restriction enzymes with different sensitivity to single stranded regions, ribonucleotides, methylation modifications and sequence contexts were selected to capture different types of modifications. All together 17 recognition sites for TaqI, AluI, HpaII and MspI in the mtDNA were selected for further analyses. TaqI and AluI recognize TCGA and AGCT sequences, respectively, and are sensitive to combinations of 6-methyladenine. HpaII and MspI recognize CCGG sequences, and are distinctly sensitive to positions of 5-methylcytosine or alternatively 5-hydroxymethylcytosine. In addition, HpaII is highly sensitive to sequence variations and reaction conditions and thereby enables sensitive quantitation of DNA alterations [14]. The sites were positioned in three mtDNA genes; the *mt-Rnr1* (12S), *mt-Nd1* (Nd1) and *mt-Cox1* (Cox1). The first TaqI site is termed T1, second AluI site A2 and so forth (Figure 1).

First, heart mtDNA from young (6-8 months) wild type (WT) mice was selected as reference genome for further comparison of mtDNA of different origins. It was found that frequency of modifications in the reference mtDNA differed considerably between the 17 sites, from 0.04 % in T1 to 13.8 % in H3 (Figure 1A). The sites also vary within the same amplicons, for instance is modification level in the A1 site four times higher than that in the M1 site. The highest signals were obtained in the HpaII and AluI sites, while the TaqI sites were least modified as judged from the cleavage efficiency. A different mtDNA modification pattern was found when mtDNA from MEF cells was analysed (Figure 1B). Here, modifications between sites were less variable, except for the T1 and A2/A3 sites. The cumulative modification levels (sum of modifications in all sites) were similar in MEF mtDNA and heart mtDNA (reference), demonstrating that the difference cannot be ascribed to DNA damage load. To further evaluate sensitivity to batch variations, we determined the relative modification level in a site (site modification divided by the sum of modifications in all sites). Figure 1C shows the relative modification level for reference mtDNA (young heart mtDNA), and Figure 1D the corresponding pattern for MEF mtDNA. The coefficient of variation was relatively similar in A and C (as in B and D), implying that variations between DNA isolates did not exert a major impact on the deviations.

The results demonstrate that heart and MEF mtDNA have site-specific modifications that can be used to distinguish heart from MEFs.

We then compared the modification pattern in reference mtDNA with mtDNA from two other post-mitotic tissues: liver and brain. Relative to reference mtDNA, the H1 and H4 sites in brain mtDNA were less modified, while the H6 was more modified. Liver mtDNA was more modified in the sites M1, H2, M2, T2, H3 and M3, but less in the H3 and H4 sites ($p<0.003$). Table 4 provides an overview of site difference. It became apparent that 3 sites (A1, A3 and H5) are similar in all tissues while the remaining sites display tissue specific patterns. For instance, the modification of the Cox1 site H4 appears to be specific to heart tissue as the site contribution is altered in all other situations.

When MEF mtDNA was compared with reference mtDNA, the H1, M1, H3, A2 and H4 were largely distinct (Figure 1F). mtDNA from embryonic stem cells (ES) were included to test the idea that differentiation lineage might contribute to the modification pattern. In general, the ES mtDNA displayed a modification pattern that mimicked MEF mtDNA except for some selected sites, suggesting that lineage is a less likely determinant for mtDNA modification than perhaps proliferation capacity. Oxidative stress has previously shown to modify mtDNA [12]. Given the impact of tissue type on modification pattern, we re-evaluated the effect of hydrogen peroxide treatment on modifications in all 17 sites (Figure 1F). Hydrogen peroxide induced a different mtDNA modification in sites H1, T1, M2, A2, H4, M4, A3, H5 and M5. Importantly, 8 sites did not respond to peroxide treatment, and the sites A1 and A2 became even less modified upon treatment, demonstrating that mtDNA modification level is not generally increased by peroxide. Dimension reduction analyses of the modifications throughout the 17 sites unravelled that MEF mtDNA clustered closer to tissue mtDNA than to ES mtDNA (Figure 6D). Interestingly, mtDNA from hydrogen peroxide-treated MEFs was shifted in the ES mtDNA direction (upwards in Figure 6D), suggesting that ES mtDNA shares features of oxidized intracellular conditions.

To investigate the impact of mitochondrial enzymes on site-specific modifications, brain, liver and heart mtDNA were analysed from young mice with defective ALKBH7 and OGG1 functions (Figure 2A and B, respectively). ALKBH7 has previously been shown to have altered mitochondrial function [10], and the OGG1 protein is essential for removal of 8-oxoguanine from mtDNA [6]. Genotype-specific effects were observed in *alkbh7*$^{-/-}$ brain mtDNA and in *ogg1*$^{-/-}$ mtDNA (all tissues) (Compare Figure 2A and 2B with Figure 1E, and

see Table 4). For instance, for brain H4 and T1 were differently modified in both *alkbbh7*$^{-/-}$ and *ogg1*$^{-/-}$ brain mtDNAs as compared to WT mtDNA.

3.2. Age influences mtDNA modifications in an OGG1- and ALKBH7-dependent manner

The content of mitochondrial 8-oxoguanine increases with age in rodents [18] implying that increases in mtDNA modification levels are expected in 10-11 months old animals, termed adults, compared to the young mice. Figure 3A shows the average change in the modification level in the 17 sites of adult heart mtDNA compared to young heart mtDNA. The alterations that reached statistical significance are shown in Figure 3B. Included in Figure 3B are additionally the corresponding age-dependent changes in brain and liver mtDNA from WT mice. While modifications in 3 sites in heart tissue and 7 sites in brain tissue increased with age in WT, liver tissue was not significantly affected. The same sites are presented for *alkbh7*$^{-/-}$ and *ogg1*$^{-/-}$ in Figures 3C and D, respectively. In contrast to WT liver mtDNA, ALKBH7-deficient liver mtDNA was significantly affected by age. In total were 14 sites altered significantly in mtDNA with age in *alkbh7*$^{-/-}$ mice: H2, H4, H5 and H6 in brain; H1 and M1 in heart; and all sites except A1, M3 and M5 in liver. In addition, 2 sites in heart and 4 sites in brain were also altered. PCA analyses indicated that age had a strong impact on mtDNA in the *alkbh7*$^{-/-}$ (Supplementary Figure S3). Surprisingly, the mtDNA from *ogg1*$^{-/-}$ mice did not show any age effect in any of the sites in any tissue (Figure 3D, Table 4). In support of the site-specific effect of age, the cumulative mtDNA modification level for all 17 sites was higher in the adult WT and *alkbh7*$^{-/-}$ mice, but not in adult *ogg1*$^{-/-}$ mice, compared to young mice (Supplementary Figure S1). An overview of all the 17 site modifications with age for each genotype is provided in Supplementary Figure S2.

3.3. mtDNA modifications accumulate in a mitochondrial metabolism-dependent manner

The impact of genotype and cell type is indicative of intramitochondrial metabolic processes being responsible for establishing the mtDNA modification pattern. To test whether metabolic alterations could rapidly establish a distinct mtDNA modification profile, isolated mitochondria were energized *in vitro* with complex I (pyruvate+malate: PM) or complex II substrates (Succinate: Succ) supplied with either ADP or menadione; a redox cycler known to generate superoxide anion. Mitochondria were isolated from heart and liver from WT, *alkbh7*$^{-/-}$ and *ogg1*$^{-/-}$ mice. As shown in Figure 4A and B, WT mtDNA became modified in a tissue-specific manner upon energization with different substrates. Young WT mitochondria in general responded stronger to energization. While complex I and complex II/ADP activation

induced distinct effects on liver mtDNA, heart mitochondria responded more synchronous to the different complex activations (Figure 4B).

mtDNA from *alkbh7*$^{-/-}$ hearts displayed a much more heterogeneous modification profile than corresponding WT mtDNA. Upon complex II/ADP activation the principle component 1 for liver mtDNA responded stronger than during complex I/ADP activation. ALBH7-deficient heart mtDNA did not display similar divergence (Figure 4C and D).

In general, mtDNA from *ogg1*$^{-/-}$ liver and heart were highly different, and clustered as two separate groups, where principle component 1 was mainly responsible for the separation. Importantly, compared to nontreated mitochondria, energization exerted in general different effects on mtDNA modification as compared to WT and *alkbh7*$^{-/-}$ mtDNA modification (Figure 4E and F).

In summary, the energizations therefore affected the mtDNA in a genotype- and tissue (cell type) specific manner. Importantly, while mtDNA from MEF undergoing peroxide treatment clustered upwards in the PCA plot (principle component 2; Figure 6D), different substrate manipulations mainly affected principle component 1 (compare Figure 4 B, D and F with Figure 6D). The results also show that the modifications are rapidly induced in actively respiring mitochondria within the 20 minutes, and form another modification profile than obtained by oxidation treatment.

3.4. Possible impact of ribonucleotides and cytosine methylation on mtDNA modification pattern

To investigate more on the possible underlying cause of the mtDNA modifications, the ability of the four selected restriction enzymes to cleave various nucleic acid substrates containing modified nucleotides was re-assessed. Figure 5A provides an overview of the different sequence contexts that are reported to occur in mtDNA and that were used to test the restriction enzymes. The most efficient TaqI restriction enzyme cleaved all DNA substrates, and to some extent also RNA-DNA heteroduplex, while AluI was efficiently inhibited by both single stranded DNA and RNA (Figure 5B). As shown in Figure 5C, HpaII was inhibited by all combinations of modifications and strictly required double stranded DNA substrate. In contrast, the isoform MspI tolerated single stranded substrate when not modified, as well as single methylated duplex DNA (Figure 5D). These results agree with the above findings

(Figure 1 and 2) that the estimated level of modifications in the TaqI sites is indicative of a strong restriction enzyme activity towards various modifications. In view of the sensitivity profiles (Figure 5B-D), ongoing transcription could be responsible for the modification signal. However, the levels of the three transcripts (12S, Nd1 and Cox1) did not correlate with the modification signals (Figure 5E).

The impact of ribonucleotides was investigated more closely. DNA from young male heart (reference mtDNA) was treated with $RNaseI_f$ to remove ribonucleotides prior to analyses. This resulted in a dramatic reduction in the modification level (Figure 6A) and suggested that RNA indeed contributes to the modification signal. However, when the relative modification profile was determined (as in Figure 1C), it became evident that although RNA contributed to the level of modification, it appeared not to dictate the distribution of modifications along the 17 sites (Figure 6B). We then evaluated the effect of RNase treatment on MEF mtDNA (Figure 6C), where MspI, AluI and TaqI cleavage efficiency increased in general (reduced the modification level). Hydrogen peroxide treatment of cells made mtDNA more resistant to cleavage, while RNase pretreatment reversed this resistance for TaqI and AluI enzymes (Figure 6E). RNase pretreatment did not have a major impact on MspI/HpaII activity. The mtDNA modifications were further evaluated by PCA (before and after RNase treatment) for reference (wt-h) and adult heart (wt-H) mtDNA (Figure 6D). It was observed that the RNase treatment affected principle component 2 more than principle component 1, similarly as hydrogen peroxide treatment. This observation alludes to that oxidative DNA damage somehow associates with ribonucleotides in mtDNA. The T1 and T2 sites are particularly important to evaluate ribonucleotide, as TaqI enzyme is sensitive to RNA-DNA but none of the other tested substrates (Figure 5). The combined effects of RNase on AluI and TaqI can be explained by RNA-DNA being converted to double stranded DNA substrate (Figure 5). The RNase also exerted a strong effect on MspI, AluI and TaqI efficiency on mtDNA from nontreated cells as well (Figure 6E), inferring that ribonucleotides are not restricted to oxidative stress assignment.

3.5. Nuclear DNA modification is different from mtDNA modification

We previously found that damage to nuclear DNA was induced in a site-specific manner [12]. In order to investigate if the modification dependence discovered for mtDNA is valid for nuclear DNA as well, a sequence in the *Gapdh* gene containing all recognition sites closely positioned were analysed (Figure 7). In the four selected sites, there was no indication of increased modification of age in nuclear DNA from heart (Figure 7A). When comparing brain

and liver from young and adult mice, the effect of age was absent except for an increased signal produced by the HpaII enzyme originating from the adult female cohort. Principle component analysis indicated relative clustering of the heart and brain nuclear DNA, while nuclear DNA from liver and ES/MEF cells differed (Figure 7C). Pretreatment with RNase to remove RNA did not alter the principal components, indicating that RNA does not contribute to modification pattern of nuclear DNA (Figure 7D).

3.7. mtDNA modifications do not influence mtDNA integrity

In nuclear DNA, DNA damage causes nucleotide misincorporation by replicating polymerases with the chance of manifesting into mutations. Likewise, mtDNA modifications might in turn drive mtDNA mutagenesis that ultimately results in altered mitochondrial function and thereby produce the metabolic phenotypes of the animal models tested here. To test the possibility that mtDNA mutations underlie some of the mtDNA modifications, the frequencies of mutated TaqI restriction enzyme sites were determined. TaqI is resistant to single stranded DNA and ribonucleotide (Figure 5B) and have successfully been used to quantify the frequency of mutations in mtDNA [17, 19]. The mtDNA mutation frequencies in the T1 site was previously found to be lower than in the T2 site, as well as differing approximately two-fold between 1 and 18 months of age [17]. This was confirmed here (Figure 8A). Interestingly, mtDNA mutation frequency appeared to increase dramatically in the adult *alkbh7*$^{-/-}$ mice. However, there was no correlation between mtDNA mutation frequency and mtDNA modification levels (Figure 8B). In contrast, the mtDNA modification levels in the T1 site correlated with those in the T2 ($r=0.92$, $p<0.001$) (Figure 8C) and accordingly, mutation frequencies in the two sites correlated significantly ($r=0.83$, $p<0.001$) (Figure 8D). The situation was similar for the specific genotypes as well. Thus, modification of mtDNA does not impact mtDNA mutagenesis and therefore is unlikely to influence the mutation frequency of the mitochondrial genome.

4. Discussion

In the current study, we show that mtDNA rapidly responds to metabolic processes. Different tissues and genotypes, as well as age were characterized by distinct patterns of mtDNA modifications. It was found that the mitochondrial OGG1 and ALKBH7 proteins contributed

to mtDNA modifications. Importantly, OGG1 strongly mediates the age-mediated modification of mtDNA.

The conditions that were addressed in this study were chosen because they were either known to alter mitochondrial function, as exemplified by altered biochemical complex activity with age [20], the increased mitochondrial respiration capacity in *alkbh7*$^{-/-}$ liver [10], metabolic phenotype of the *ogg1*$^{-/-}$ and *alkbh7*$^{-/-}$ mice [7, 10], or because they influence mtDNA integrity like tissue-specific copy number and mtDNA repair capacity [21, 22]. One implication from our finding is that tissue specificity, mtDNA repair capacity and mitochondrial function correlate with mtDNA modifications, which in turn mirrors the mitochondrial identity.

Although we have not unravelled the molecular mechanisms determining the pattern of modifications, the results imply that RNA constitutes an important contributor. Interestingly, removal of RNA reduced the modification signals but did not alter the modification profile of the mtDNA. One interpretation of this finding is that the amount of mitochondrial RNA determines the amplitude of the signal. Two peculiar findings from these experiments are important: first, the RNase-sensitive signal increased with age, and second, exposure of cells to sublethal doses of hydrogen peroxide increased the level mtDNA modifications that include RNA. Together, these observations suggest that oxidative damage to mtDNA accumulates with age and that this in turn triggers mitochondrial RNA synthesis. The purpose of this RNA synthesis is under current investigation, but it appears that mtDNA repair play an important role, as demonstrated by the absent age-effect on the modification level in OGG1-deficient animals.

Analyses of mtDNA from OGG1-deficient mitochondria demonstrated a characteristic mtDNA modification profile different from that of WT mtDNA. Thus, although mtDNA from *ogg1*$^{-/-}$ mice was resistant to age-mediated modifications analysed here, one possible explanation for the genotype effect could be that OGG1 functions to mediate metabolism-induced mtDNA modifications, independent of age. In favour of this hypothesis is the fact that mtDNA in isolated mitochondria from *ogg1*$^{-/-}$ mice that were energized *in vitro* became differently modified compared to WT mtDNA under similar treatments.

For energization of mitochondria *in vitro*, twenty minutes was sufficient to alter the mtDNA as indicated by the PCA parameters (Figure 4), primarily because of principle component 1. In comparison, 15 min exposure to hydrogen peroxide induced another mtDNA modification

pattern, mainly affecting principle component 2. The same principle component distinguished cell type and cell/tissue specificity. These results imply that metabolic-mediated modifications and cell type/oxidative stress-mediated modifications are distinct factors that influence mtDNA. The positioning in the PCA plot suggests that mitochondrial redox levels in ES cells are more oxidative than in MEFs and tissue, which is partly contradictory to established views. The other explanation is that the maintenance of mtDNA from ES, MEFs and postmitotic tissue differs.

In this paper, 17 different sites representing less than 0.1% of the total mtDNA were investigated, suggesting that modifications can occur everywhere in the mtDNA, and thus be a very important feature of the mtDNA biology. The molecular explanation is possibly linked to the organization of mtDNA into tight assemblies with metabolic proteins, proteins from fatty acid oxidation and members of oxidative decarboxylation complexes that are classified as nucleoid members [5, 23]. Importantly, many metabolic complexes (as e.g. pyruvate dehydrogenase) generate superoxide that can exceed the ETC-mediated superoxide production from complex I [24, 25]. The mitochondrial nucleoid wraps up mtDNA in a metabolism-dependent manner [26], and studies of various cells and tissues [5, 27-29] imply that the nucleoid has a tissue-specific composition that modifies the mtDNA in a mitochondrion-specific manner.

The impact of OGG1 in forming the mtDNA modification profile combined with the metabolic profile of OGG1-deficient animals infers that the modification of mtDNA is not only a secondary feature of ongoing metabolism, but may also serve to regulate metabolic processes. Classically, functional impact of mtDNA modifications is attributed to mitochondrial epigenetics, and although there are several reports of CpG- and non-CpG methylation of mtDNA, many of the applied methods are associated with false signals [14]. However, although some mtDNA modifications can be ascribed to cytosine methylation, the modifications identified in recognition sites of cytosine methylation-resistant restriction enzymes (Table 4) suggest that other types of molecular signals serve epigenetic features. It is interesting to note that aconitase, a ROS-sensitive/sensor intramitochondrially is stabilized by mitochondrial OGG1 in an repair-independent manner [30].

Here, *alkbh7*$^{-/-}$ mice were included with the purpose to investigate potential effect on mtDNA modification level. Although ALKBH7 paralogues have DNA repair activities, the mitochondrial ALKBH7 does not necessarily act on mtDNA. Initial characterizations implied a role of ALKBH7 in fatty acid oxidation and metabolic regulation. In view of ALKBH7's

role in energized mitochondria, it is possible that metabolic alterations formed the mtDNA modifications characteristic of the mutant's mitochondrial activity. While modifications in the mtDNA from the *ogg1*$^{-/-}$ was resistant to age, the *alkbh7*$^{-/-}$ mtDNA appears in general to be more responsive (Table 4), perhaps an indication of the higher mitochondrial respiration capacity in the mutant [10].

The principal component analyses enabled a closer identification of the sites whose contributions determined the size of component 1, which represented more than 90% of the variations. To distinguish between tissues, the contributions from sites A1, A2 and A3 were typically shifted to negative values (from close to +1). E.g. reference tissue was classified by positive contributions from all sites (with more than 0.9 in weight), liver mtDNA had a component with negative values in A1, A2 and A3. In brain, A1 and A2 were negative, in addition to H3 and H4. Age, on the other hand appeared to be linked to an additional change in M5 and M6 sites. OGG1 deficiency exerted a different contribution to the sites T1 and T2 (liver), and M1 and M3, H4 and H6 (brain, heart). ALKBH7 deficiency demonstrated an altered contribution to sites T1,T2,H5 and M6. Thus, while the AluI exerted stringencies in the components to separate WT tissues and age, MspI and TaqI sites were more frequent in the mutants. These were again selective against RNA-DNA and ssDNA substrate contexts (Figure 5B). Isolated mitochondria energized with pyruvate/malate in the presence of ADP had a negative contribution factor to T1 and M5 compared to energization without ADP. Succinate energization exerted a different effect on the component, mainly due to negative contribution from the sites H1, T1-H3, H4, M4 and H6 (for liver mitochondria). In heart mitochondria, a similar pattern was apparent. Thus, in summary, while AluI sites seem to determine tissue and genotype specificity by the first component, they appeared to have lower impact on shaping mtDNA modifications during energization of isolated mitochondria. On the other hand, HpaII sensitivity appears to be more discriminative for the energization. HpaII is known to be sensitive to sequence contexts, suboptimal reaction conditions, in addition to methylation [14].

Correlation analyses allowed us to conclude that mtDNA modifications that are characteristic of metabolism, as well as that they do not influence mtDNA mutation frequency. This is supported by the normal mtDNA mutation frequency in the mtDNA repair double mutant *ogg1*$^{-/-}$ */myh*$^{-/-}$ [20]. Biochemical studies have indicated that mtDNA mutation frequency is merely a side effect of (sequence-dependent) misincorporation by DNA pol γ, rather than as being caused by mispairing of accumulating, premutagenic base lesions in the mDNA [31,

32]. The obvious question is then why the cell harbours a mtDNA repair system if it is not to protect against mutagenesis. Ectopic overexpression of OGG1 protects cells against elevated oxidative stress, support normal neuronal biogenesis and secures mitochondrial maturation during stem cell differentiation [33-35]. In view of the present data, it cannot be ruled out that the survival effect is due to metabolic regulation rather than cytotoxic effects of unrepaired mtDNA lesions. Emerging results imply that the cellular role of mtDNA repair is closer associated to metabolic regulation than survival [7, 36].

Supplemental data

Supplemental data include Figure S1-S3.

Acknowledgement

The study was supported by grants from the University of Oslo. We are grateful to Rajikula Suganthan and Guro Flor Lien for the mouse tissue dissection.

Conflict of interest

The authors declare no conflict of interest

REFERENCES

[1] N.C. Souza-Pinto, D.L. Croteau, E.K. Hudson, R.G. Hansford, V.A. Bohr, Age-associated increase in 8-oxo-deoxyguanosine glycosylase/AP lyase activity in rat mitochondria, Nucleic Acids Res, 27 (1999) 1935-1942.

[2] E.K. Hudson, B.A. Hogue, N.C. Souza-Pinto, D.L. Croteau, R.M. Anson, V.A. Bohr, R.G. Hansford, Age-associated change in mitochondrial DNA damage, Free Radic Res, 29 (1998) 573-579.

[3] F.M. Yakes, B. Van Houten, Mitochondrial DNA damage is more extensive and persists longer than nuclear DNA damage in human cells following oxidative stress, Proc Natl Acad Sci U S A, 94 (1997) 514-519.

[4] D.F. Bogenhagen, Mitochondrial DNA nucleoid structure, Biochim Biophys Acta, 1819 (2012) 914-920.

[5] D.F. Bogenhagen, Y. Wang, E.L. Shen, R. Kobayashi, Protein components of mitochondrial DNA nucleoids in higher eukaryotes, Mol Cell Proteomics, 2 (2003) 1205-1216.

[6] N.C. de Souza-Pinto, L. Eide, B.A. Hogue, T. Thybo, T. Stevnsner, E. Seeberg, A. Klungland, V.A. Bohr, Repair of 8-oxodeoxyguanosine lesions in mitochondrial dna depends on the oxoguanine dna glycosylase (OGG1) gene and 8-oxoguanine accumulates in the mitochondrial dna of OGG1-defective mice, Cancer Res, 61 (2001) 5378-5381.

[7] H. Sampath, V. Vartanian, M.R. Rollins, K. Sakumi, Y. Nakabeppu, R.S. Lloyd, 8-Oxoguanine DNA glycosylase (OGG1) deficiency increases susceptibility to obesity and metabolic dysfunction, PLoS One, 7 (2012) e51697.

[8] M. Scheibye-Knudsen, S.J. Mitchell, E.F. Fang, T. Iyama, T. Ward, J. Wang, C.A. Dunn, N. Singh, S. Veith, M.M. Hasan-Olive, A. Mangerich, M.A. Wilson, M.P. Mattson, L.H. Bergersen, V.C. Cogger, A. Warren, D.G. Le Couteur, R. Moaddel, D.M. Wilson, 3rd, D.L. Croteau, R. de Cabo, V.A. Bohr, A high-fat diet and NAD(+) activate Sirt1 to rescue premature aging in cockayne syndrome, Cell Metab, 20 (2014) 840-855.

[9] S. Azam, N. Jouvet, A. Jilani, R. Vongsamphanh, X. Yang, S. Yang, D. Ramotar, Human glyceraldehyde-3-phosphate dehydrogenase plays a direct role in reactivating oxidized forms of the DNA repair enzyme APE1, J Biol Chem, 283 (2008) 30632-30641.

[10] A. Solberg, A.B. Robertson, J.M. Aronsen, O. Rognmo, I. Sjaastad, U. Wisloff, A. Klungland, Deletion of mouse Alkbh7 leads to obesity, J Mol Cell Biol, 5 (2013) 194-203.

[11] V.K. Mootha, J. Bunkenborg, J.V. Olsen, M. Hjerrild, J.R. Wisniewski, E. Stahl, M.S. Bolouri, H.N. Ray, S. Sihag, M. Kamal, N. Patterson, E.S. Lander, M. Mann, Integrated analysis of protein composition, tissue diversity, and gene regulation in mouse mitochondria, Cell, 115 (2003) 629-640.

[12] J.M. Strand, K. Scheffler, M. Bjoras, L. Eide, The distribution of DNA damage is defined by region-specific susceptibility to DNA damage formation rather than repair differences, DNA Repair (Amst), 18 (2014) 44-51.

[13] M.W. Schmitt, S.R. Kennedy, J.J. Salk, E.J. Fox, J.B. Hiatt, L.A. Loeb, Detection of ultra-rare mutations by next-generation sequencing, Proc Natl Acad Sci U S A, 109 (2012) 14508-14513.

[14] T. Pawar, L. Eide, Pitfalls in mitochondrial epigenetics, Mitochondrial DNA A DNA Mapp Seq Anal, (2016) 1-10.

[15] D.L. Croteau, C.M. ap Rhys, E.K. Hudson, G.L. Dianov, R.G. Hansford, V.A. Bohr, An oxidative damage-specific endonuclease from rat liver mitochondria, J Biol Chem, 272 (1997) 27338-27344.

[16] W. Wang, K. Scheffler, Y. Esbensen, L. Eide, Quantification of DNA Damage by Real-Time qPCR, Methods Mol Biol, 1351 (2016) 27-32.

[17] W. Wang, K. Scheffler, Y. Esbensen, J.M. Strand, J.B. Stewart, M. Bjoras, L. Eide, Addressing RNA integrity to determine the impact of mitochondrial DNA mutations on brain mitochondrial function with age, PLoS One, 9 (2014) e96940.

[18] M. Lopez-Torres, R. Gredilla, A. Sanz, G. Barja, Influence of aging and long-term caloric restriction on oxygen radical generation and oxidative DNA damage in rat liver mitochondria, Free Radic Biol Med, 32 (2002) 882-889.

[19] M. Vermulst, J.H. Bielas, G.C. Kujoth, W.C. Ladiges, P.S. Rabinovitch, T.A. Prolla, L.A. Loeb, Mitochondrial point mutations do not limit the natural lifespan of mice, Nat Genet, 39 (2007) 540-543.
[20] R. Halsne, Y. Esbensen, W. Wang, K. Scheffler, R. Suganthan, M. Bjoras, L. Eide, Lack of the DNA glycosylases MYH and OGG1 in the cancer prone double mutant mouse does not increase mitochondrial DNA mutagenesis, DNA Repair (Amst), 11 (2012) 278-285.
[21] B. Karahalil, B.A. Hogue, N.C. de Souza-Pinto, V.A. Bohr, Base excision repair capacity in mitochondria and nuclei: tissue-specific variations, FASEB J, 16 (2002) 1895-1902.
[22] K.L. Veltri, M. Espiritu, G. Singh, Distinct genomic copy number in mitochondria of different mammalian organs, J Cell Physiol, 143 (1990) 160-164.
[23] X.J. Chen, X. Wang, B.A. Kaufman, R.A. Butow, Aconitase couples metabolic regulation to mitochondrial DNA maintenance, Science, 307 (2005) 714-717.
[24] A.A. Starkov, G. Fiskum, C. Chinopoulos, B.J. Lorenzo, S.E. Browne, M.S. Patel, M.F. Beal, Mitochondrial alpha-ketoglutarate dehydrogenase complex generates reactive oxygen species, J Neurosci, 24 (2004) 7779-7788.
[25] C.L. Quinlan, R.L. Goncalves, M. Hey-Mogensen, N. Yadava, V.I. Bunik, M.D. Brand, The 2-oxoacid dehydrogenase complexes in mitochondria can produce superoxide/hydrogen peroxide at much higher rates than complex I, J Biol Chem, 289 (2014) 8312-8325.
[26] M. Kucej, B. Kucejova, R. Subramanian, X.J. Chen, R.A. Butow, Mitochondrial nucleoids undergo remodeling in response to metabolic cues, J Cell Sci, 121 (2008) 1861-1868.
[27] X.J. Chen, X. Wang, R.A. Butow, Yeast aconitase binds and provides metabolically coupled protection to mitochondrial DNA, Proc Natl Acad Sci U S A, 104 (2007) 13738-13743.
[28] Y. Wang, D.F. Bogenhagen, Human mitochondrial DNA nucleoids are linked to protein folding machinery and metabolic enzymes at the mitochondrial inner membrane, J Biol Chem, 281 (2006) 25791-25802.
[29] D.F. Bogenhagen, D. Rousseau, S. Burke, The layered structure of human mitochondrial DNA nucleoids, J Biol Chem, 283 (2008) 3665-3675.
[30] V. Panduri, G. Liu, S. Surapureddi, J. Kondapalli, S. Soberanes, N.C. de Souza-Pinto, V.A. Bohr, G.R. Budinger, P.T. Schumacker, S.A. Weitzman, D.W. Kamp, Role of mitochondrial hOGG1 and aconitase in oxidant-induced lung epithelial cell apoptosis, Free Radic Biol Med, 47 (2009) 750-759.
[31] W.C. Copeland, Defects in mitochondrial DNA replication and human disease, Crit Rev Biochem Mol Biol, 47 (2012) 64-74.
[32] W. Zheng, K. Khrapko, H.A. Coller, W.G. Thilly, W.C. Copeland, Origins of human mitochondrial point mutations as DNA polymerase gamma-mediated errors, Mutat Res, 599 (2006) 11-20.
[33] A.W. Dobson, V. Grishko, S.P. LeDoux, M.R. Kelley, G.L. Wilson, M.N. Gillespie, Enhanced mtDNA repair capacity protects pulmonary artery endothelial cells from oxidant-mediated death, Am J Physiol Lung Cell Mol Physiol, 283 (2002) L205-210.
[34] W. Wang, P. Osenbroch, R. Skinnes, Y. Esbensen, M. Bjoras, L. Eide, Mitochondrial DNA integrity is essential for mitochondrial maturation during differentiation of neural stem cells, Stem Cells, 28 (2010) 2195-2204.
[35] W. Wang, Y. Esbensen, D. Kunke, R. Suganthan, L. Rachek, M. Bjoras, L. Eide, Mitochondrial DNA damage level determines neural stem cell differentiation fate, J Neurosci, 31 (2011) 9746-9751.
[36] H. Sampath, A.K. Batra, V. Vartanian, J.R. Carmical, D. Prusak, I.B. King, B. Lowell, L.F. Earley, T.G. Wood, D.L. Marks, A.K. McCullough, R.S. L, Variable penetrance of metabolic phenotypes and development of high-fat diet-induced adiposity in NEIL1-deficient mice, Am J Physiol Endocrinol Metab, 300 (2011) E724-734.

Figure legends

Figure 1. Site-specific mtDNA modification pattern varies with cell- and tissue type

The mtDNA modifications in 17 different restriction enzyme recognition sites in the *mt-Rnr1* (12S), *mt-Nd1* (ND1) and *mtCox1* (COX1) mitochondrial genes were analyzed. Quantification of mtDNA modifications was determined as described in materials and methods. (**A**) Characteristic mtDNA modification pattern for the chosen reference tissue (mtDNA from young male heart WT) as average level of modification, with SD (n=6). (**B**) Characteristic mtDNA modification pattern for MEFs as average level of modification, with SD (n=4). (**C**) Relative mtDNA modifications in heart mtDNA, young WT; same set as in (A), presented as relative contribution of the specific site to the sum of all sites, with SD. (**D**) Relative mtDNA modifications in MEF mtDNA; same set as in (B), presented as relative contribution of the specific site to the sum of all sites, with SD. (**E**) Relative site modification was calculated for brain mtDNA and liver mtDNA tissue (black and grey, respectively) from young mice. The average deviation in modification from reference (C) is presented, with SD (n=15). Brain tissue differs significantly at sites H1, H4 and H6. Liver tissue differs significantly at M1, H2, M2, T2, H3, M3 and H4 ($p<0.003$). (**F**) Relative site modification was calculated for mtDNA from three cell sources: ES cells (n=4, blue) MEF cells (n=4, black) and H_2O_2-treated MEF cells (n=3, grey bowls), and presented as average deviation, with SD. ES cell mtDNA differs significantly from reference at all sites except A1, A2, A3 and H5. MEF mtDNA differs significantly from reference at the same locations as ES cells expect for H2 and H6, and additionally at A2. H_2O_2-treatment of MEF cells diminishes the difference between ES cells and MEF cells, as the effect at A2 perishes while H2 and H6 re-emerges ($p<0.003$).

Figure 2. Site-specific mtDNA modification depends on ALKBH7 and OGG1 proteins

The mtDNA modifications in the same sites as in Figure 1 were analyzed in liver, brain and heart of *ogg1*$^{-/-}$ and *alkbh7*$^{-/-}$ mice. (**A**) Relative site modification was calculated for the indicated tissues from young ALKBH7-deficient mice and presented as average deviation from reference (Figure 1C), with SD (n= 4). **(B)** Relative site modification was calculated and presented similarly for the indicated tissue from young OGG1-deficient mice, with SD. Color codes: brain (black), heart (blue) and liver (grey) mtDNA, (n= 3).

Figure 3. OGG1 and ALKBH7 influence the effect of age on mtDNA modification

mtDNA from liver, brain and heart of adult mice (10-11 months) of WT, *ogg1*$^{-/-}$ and *alkbh7*$^{-/-}$ mice were analysed for site modifications and compared to those of young mice. (**A**) Relative site modification in mtDNA from adult WT heart calculated and presented as average deviation from that in mtDNA from young WT heart (Figure 1C), with SD (n=3). **(B)** The sites in heart mtDNA (in A) that were significantly ($p<0.003$) modified with age are presented as relative change with age. Included in the figure are additionally the relative increases with age in the corresponding sites from liver and brain mtDNA. **(C)** Sites in the mtDNA from *alkbh7*$^{-/-}$ mice that are significantly ($p<0.003$) altered with age, were presented relative to those in young mice. (**D**) Relative change in site modification with age in mtDNA from *ogg1*$^{-}$

$^{/-}$ tissues. The figure shows the results for the same sites that were significantly altered in WT mice (B). None of the sites change significantly with age in *ogg1*$^{-/-}$ mtDNA. Color codes: brain (black), heart (blue) and liver (grey).

Figure 4. Unique mtDNA modification pattern is induced in respiring mitochondria upon specific substrates *in vitro*.

mtDNA modifications in energized mitochondria from heart and liver were analysed for site modifications. (**A**) Relative site modification pattern of mtDNA from isolated mitochondria from young and adult WT mice. The results shown are average deviation from reference (Figure 1A), with SD (n = 6). (**B**) PCA score plot of energized heart (blue) and liver (grey) WT mtDNA (**C**) Relative site modification of heart (blue) and liver (grey) mtDNA from young and adult *alkbh7*$^{-/-}$ mitochondria. The results shown are average deviation from reference, with SD. (**D**) Same as (B) for *alkbh7*$^{-/-}$ mtDNA. (**E**) Same as (A) for *ogg1*$^{-/-}$ mtDNA (6 mo, n = 3) heart (blue bowls) and liver (grey bowls). (**F**) Same as (B) for *ogg1*$^{-/-}$ mtDNA. Energizations include: NT: nontreated; PM +/-ADP: pyruvate+malate +/-ADP; SUCC +/-ADP: succinate +/-ADP; PM + Men: pyruvate+malate+menadione.

Figure 5. Ongoing transcription is not causing the mtDNA modifications

The four restriction enzymes used to quantify mtDNA modifications (MspI , TaqI HpaII and AluI) were tested for the ability to act on DNA and RNA substrates and methylated cytosines. (**A**) Overview of substrates used. The substrates were prepared as described in materials and methods. 5mC: 5-methylcytosine; dsDNA:duplex oligonucleotide; ssDNA: single oligonucleotide; DNA-RNA: DNA –RNA heteroduplex oligonucleotide. (**B**) Effect of single strand and RNA on the cleavage by AluI (black) and TaqI (grey). (n=3). (**C**) Effect of single strand, 5mC and RNA on the cleavage by HpaII. (n=3). (**D**) Effect of single strand, 5mC and RNA on the cleavage by MspI. (n=3). (**E**) Comparison of relative gene expression (horizontal lines) with the corresponding site modification (bars) for reference tissue (young WT heart; n=3).

Figure 6. Ribonucleotides are introduced in mtDNA during oxidative stress but do not alter relative mtDNA modification profile

The amount of ribonucleotides in mtDNA was determined by pretreating isolated mtDNA with RNase as described in materials and methods and subsequently quantifying mtDNA modification. (**A**) Characteristic mtDNA modification pattern for the chosen reference tissue (heart mtDNA from young WT mice (n=6) before (black) and after (orange) RNase treatment. (**B**) Presentation of the relative site modifications of the same data set as in (A). (**C**) Characteristic mtDNA site modification pattern for nontreated MEF cells before (black) and after (orange) RNA removal (n=4). (**D**) PCA score plot for mtDNA modification from young and adult heart (wt-h and wt-H, respectively), ES and nontreated/peroxide-treated MEF cells (MEF/H_2O_2) with (R) and without RNAse () pretreatment, as indicated. (**E**) Characteristic mtDNA modification pattern for peroxide-treated MEF before (black) and after (orange) RNA removal (n=4).

Figure 7. Nuclear DNA does not display similar age-and tissue-dependent modification

The nuclear DNA modification was determined for the same reference material (young male WT heart) in four selected sites in the *Gapdh* gene. The figure displays how the specified tissue deviates from the reference tissue, as average deviation with SD (n=6). (**A**) Deviation in modification of selected sites in nuclear DNA from adult heart. (**B**) Deviation in modification of the same sites from young and adult liver and brain, as indicated. The figure represents average deviation from reference, with SD (adult: n=3). (**C**) PCA plot of nuclear DNA assessed by the four sites, as indicated. (**D**) PCA plot demonstrating the effect of RNase (tissue-R) on heart nuclear DNA from young and adult mice, same samples as above.

Figure 8. mtDNA modifications do not cause mtDNA mutations

mtDNA mutation frequency was determined as described in materials and methods. (**A**) Mutation frequencies in the T1 and T2 sites from of brain, liver and heart were determined and presented as mean, with SD for young and adult *alkbh7*$^{-/-}$, *ogg1*$^{-/-}$ and WT, as indicated (n=96). (**B**) Scatter plot presenting mtDNA frequencies for the corresponding mtDNA modifications in the T1 and T2 sites for all samples. (**C**) Scatter plot presenting mtDNA modifications in the T1 site versus the T2 sites. (**D**). Scatter plot presenting mtDNA mutation frequencies in the T1 versus the T2 sites.